Himawari-ANU: A recalibrated geostationary land surface temperature dataset based on MODIS spatiotemporal characteristics

#AGU23
WIDE. OPEN. SCIENCE.
San Francisco, CA & Online Everywhere
11-15 December 2023

Yi Yu [a,b,*], Luigi J. Renzullo [a,c], Tim R. McVicar [d], Thomas G. Van Niel [e], Dejun Cai [d] and Siyuan Tian [a,c]

Australian National University — Institute for Water Futures — CSIRO — DATA 61 — Centre for Entrepreneurial Agri-Technology — tern Ecosystem Research Infrastructure

[a] Fenner School of Environment & Society, The Australian National University, Canberra, ACT 2601, Australia;
[b] CSIRO Agriculture and Food, Canberra, ACT 2601, Australia; [c] Bureau of Meteorology, Canberra, ACT 2600, Australia;
[d] CSIRO Environment, Canberra, ACT 2601, Australia; [e] CSIRO Environment, Wembley, WA 6913, Australia
* Correspondence to Yi Yu (u6726739@anu.edu.au)

Introduction

- Himawari-8 satellite offers a unique opportunity to monitor sub-daily thermal dynamics over Asia and Oceania (Fig. 1).
- Inconsistency were reported between LST data obtained from geostationary and polar-orbiting platforms, particularly for daytime LST (e.g., 12 K).
- Solar Zenith Angle (SZA) serves as an ideal physical variable to quantify systematic differences between platforms.

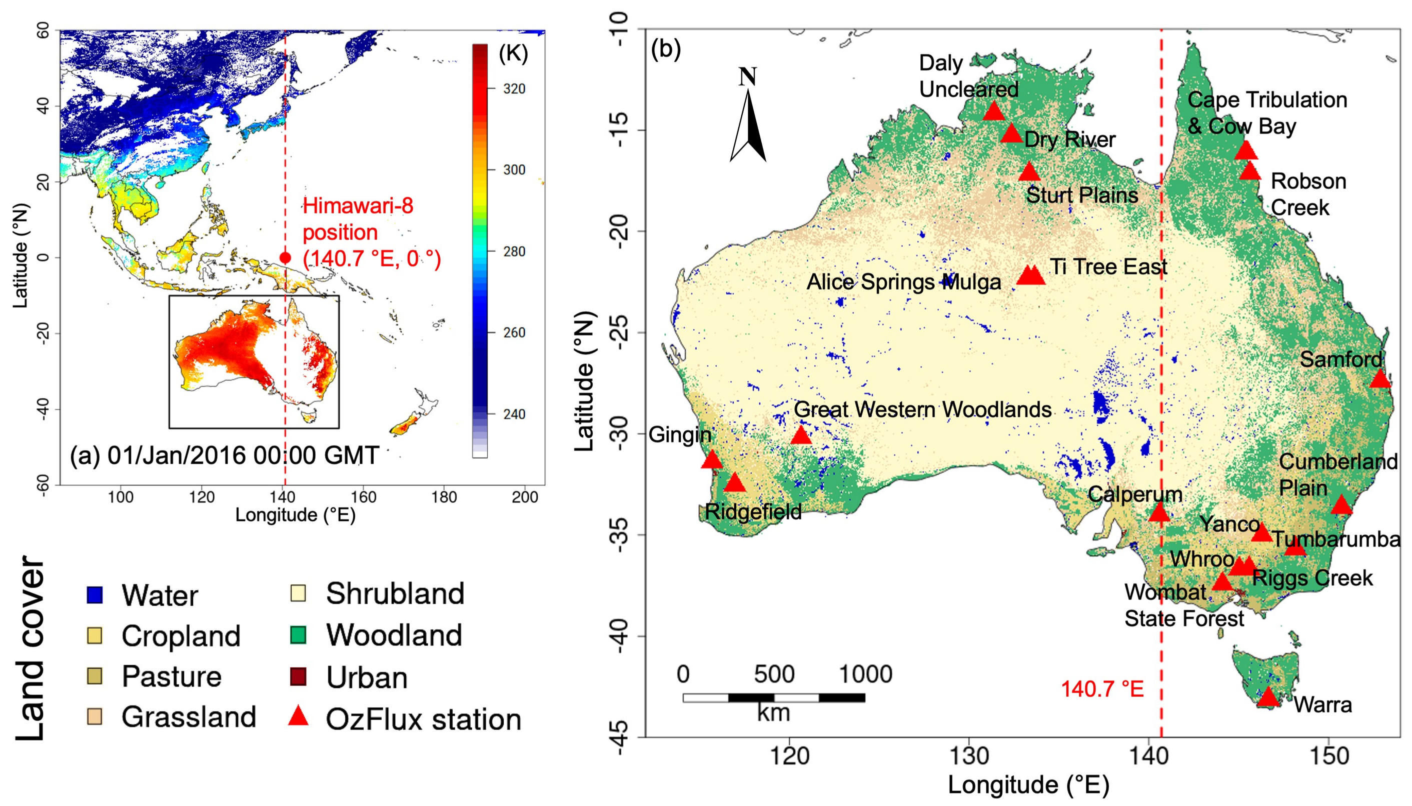

Fig. 1. (a) LST of the full-disk Himawari-8 observation area on 01/Jan/2016 00:00 GMT with clouds and oceans masked out; and (b) the land cover map of Australia and the distribution of 20 OzFlux sites.

Data and method

- $SZAC(x_i, y_i, t) = Coeff(x_i, y_i) \times log(cos\theta_{solar}(x_i, y_i, t) + 1)$
- where $SZAC$ is the calibration factor (K); (x_i, y_i) is the geolocation of a given pixel i; t is the given time; $Coeff$ is coefficient (K); θ_{solar} is SZA (°).

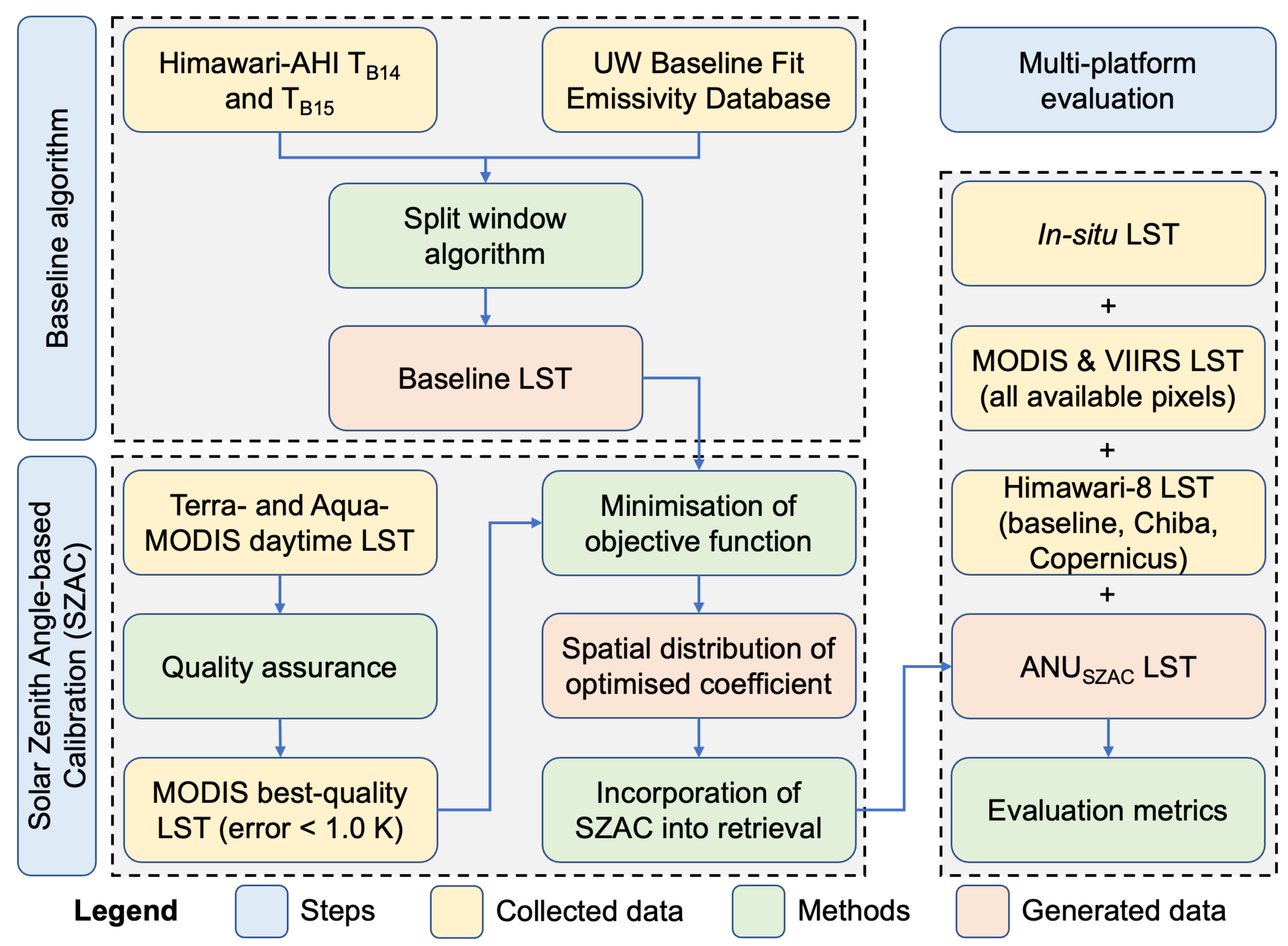

Fig. 2. Experimental design herein.

Snapshots

- SZAC variation signifies that the disparities between the baseline LST and MODIS LST were most pronounced in the summer when incoming radiation peaks and necessitate a stronger correction.
- The differences between the baseline and MODIS LST in inland and northern Australia were always higher than other regions.

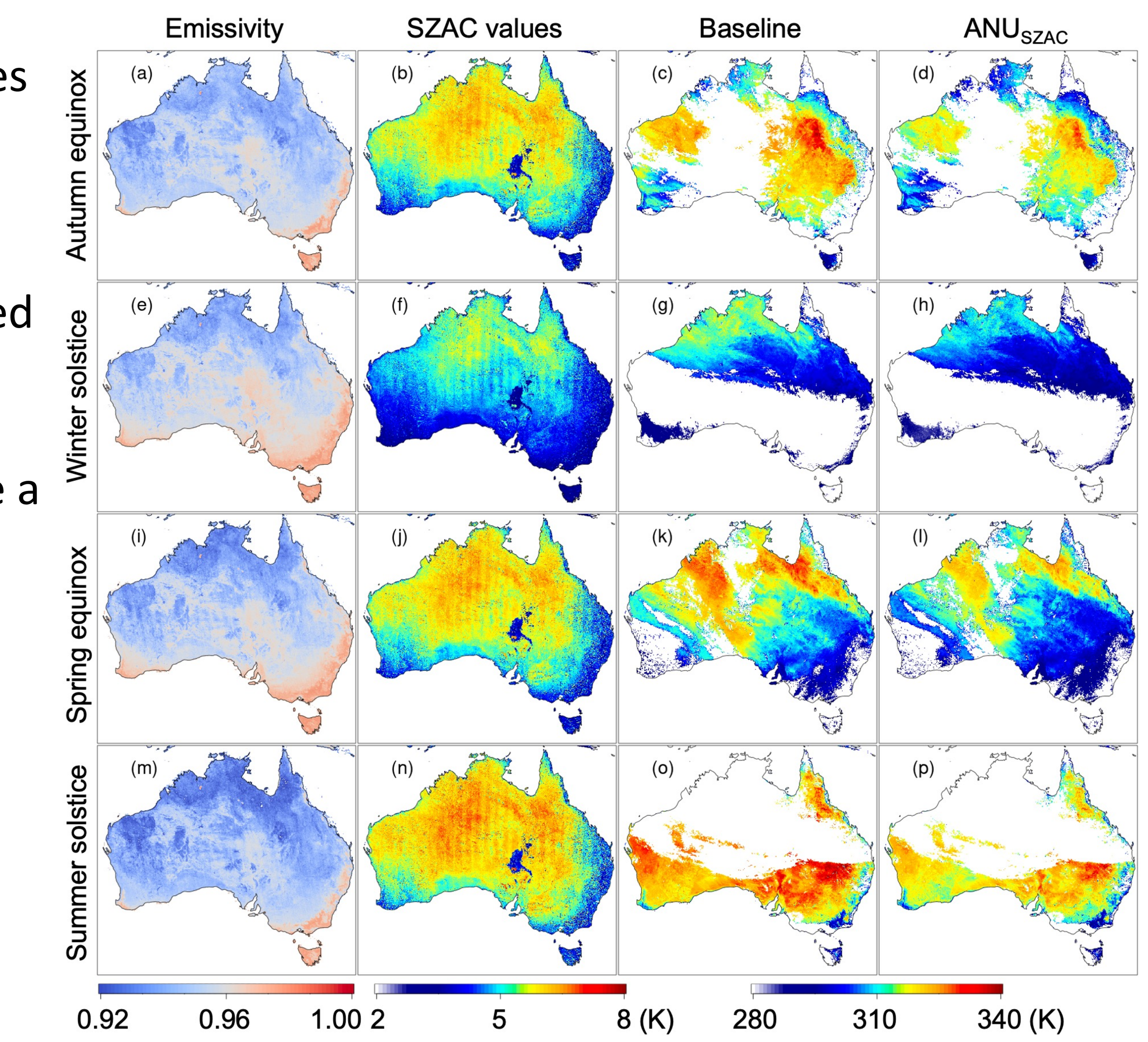

Fig. 3. Snapshots of emissivity, SZAC values, baseline and ANU_{SZAC} LST.

- Both input emissivity (Fig. 3; first column) and SZAC values (Fig. 3; second column) exhibited artefacts associated with MODIS scanning effects.

Spatial pattern of SZAC coefficient

- The SZAC coefficient revealed negative associations with vegetation cover characteristics and exhibited a greater degree of uniformity within inland regions, where calibration effects exerted a more pronounced influence (Fig. 4).
- Pixels along the eastern coastlines exhibited greater heterogeneity (Region A and C; Fig. 4 e-h and q-t), characterised by denser vegetation and relatively mountainous terrain.

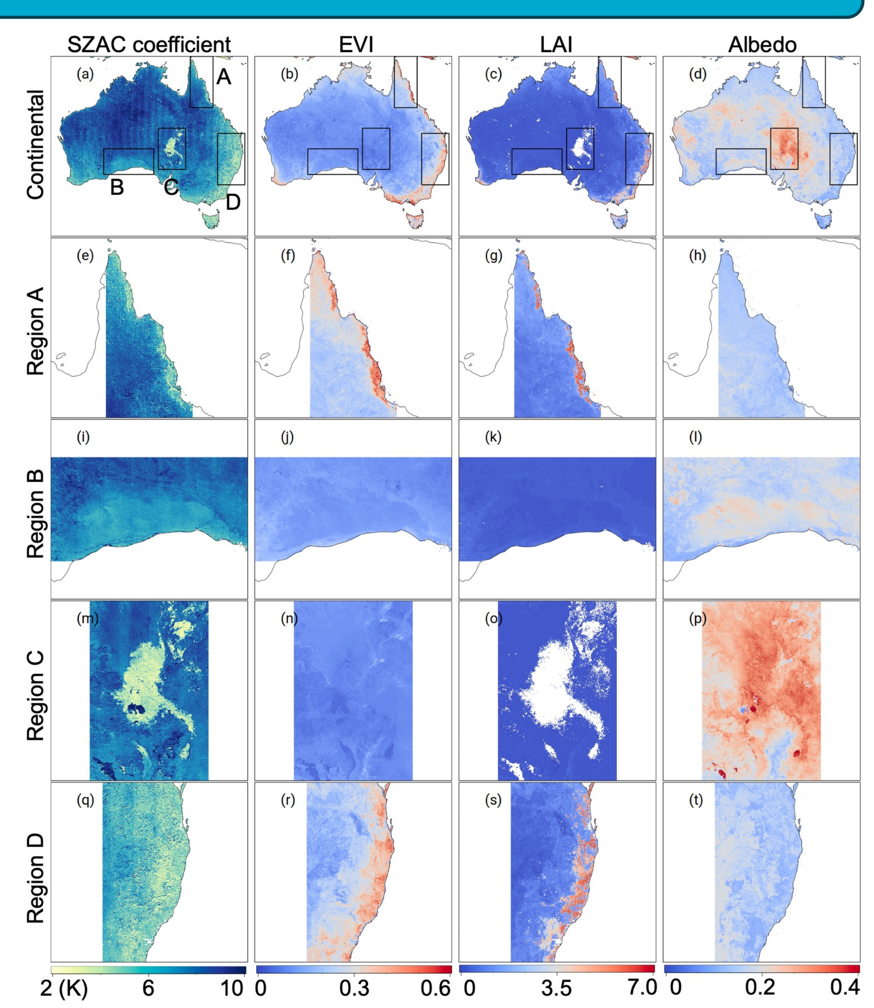

Fig. 4. (a-d) Continental-scale and (e-t) zoomed comparisons.

- For both EVI and LAI, the SZAC coefficient exhibited similar decreasing trend with increasing vegetation indices (Fig. 5).

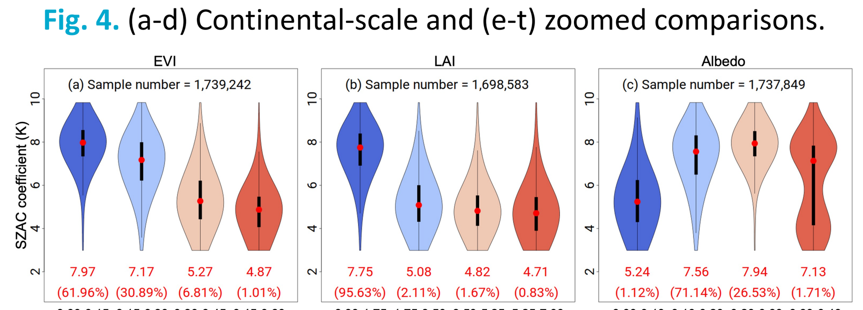

Fig. 5. Violin plots within four equal-value-range quantiles.

Cross-satellite evaluation

- The median bias (ubRMSE) of baseline, Chiba, Copernicus and ANU_{SZAC} LST against Aqua-MODIS LST for Australia was 4.85 (2.42), 2.90 (2.37), 2.28 (2.48) and 0.98 (2.44) K, respectively (Fig. 6).

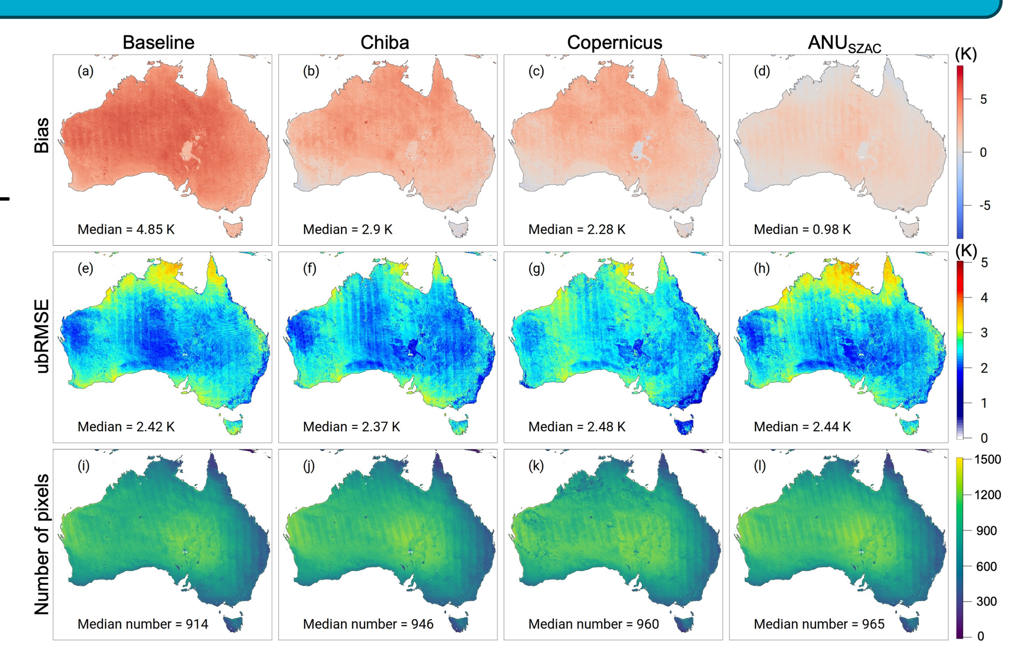

Fig. 6. Comparisons against Aqua-MODIS (i.e., MYD11A1) for Australia.

- The median bias (ubRMSE) of baseline, Chiba, Copernicus and ANU_{SZAC} LST against VIIRS LST was 3.02 (3.07), 1.07 (2.84), 0.33 (2.92) and -0.63 (2.94) K, respectively (Fig. 7).
- Both VIIRS and Aqua-MODIS have an overpass time of ~ 13:30 local solar time making this comparison essentially free of diurnal cycle influences.

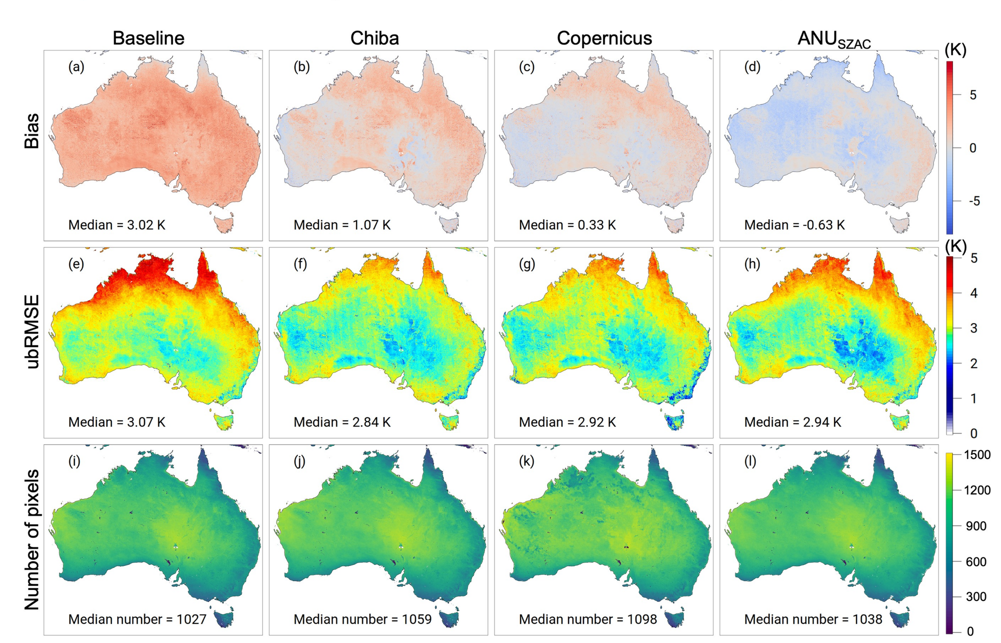

Fig. 7. Comparisons against VIIRS (i.e., VNP21A1D) for Australia.

Ground-based evaluation

- The biggest improvement in bias of ANU_{SZAC} LST was observed around midday (i.e., 10:00-12:00 local standard time; Fig. 8).

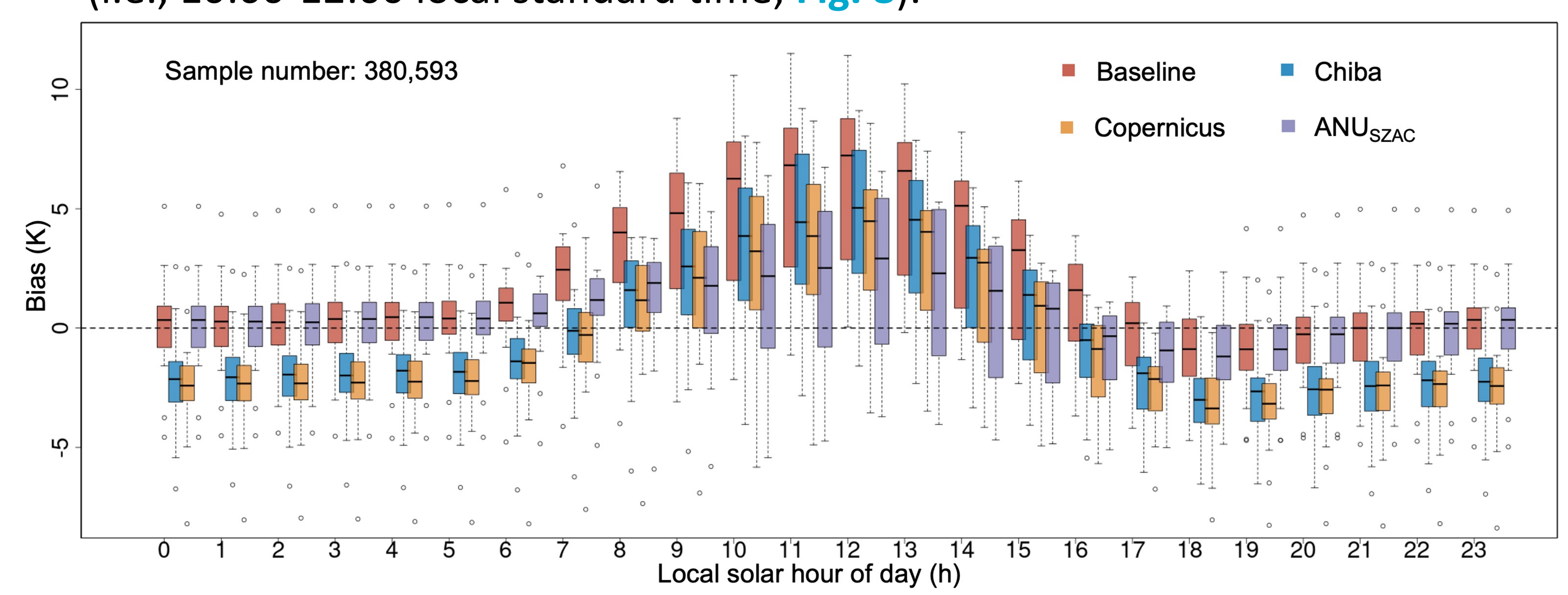

Fig. 8. Diurnal bias boxplots against OzFlux LST.

Acknowgement

This research was performed as part of a PhD by the first author (YY) under an academic collaboration between the Australian National University (ANU) and the Commonwealth Scientific and Industrial Research Organisation (CSIRO). This research was undertaken while supported by the ANU University Research Scholarship and an ANU-CSIRO Digital Agriculture PhD Supplementary Scholarship through the Centre for Entrepreneurial Agri-Technology (CEAT). We thank the ANU Institute for Water Futures for supporting this poster presentation. We thank the continued support of the TERN Landscapes Observatory (https://www.tern.org.au/tern-observatory/tern-landscapes/), a sensing platform of the Terrestrial Ecosystem Research Network (TERN; https://www.tern.org.au/), which is supported and enabled by the Australian Government through the National Collaborative Research Infrastructure Strategy (NCRIS).